environmental microbiology

Environmental Microbiology (2021) **23**(8), 4309–4325 doi:10.1111/1462-2920.15613

Genetic mapping of highly versatile and solvent-tolerant *Pseudomonas putida* B6-2 (ATCC BAA-2545) as a 'superstar' for mineralization of PAHs and dioxin-like compounds

Weiwei Wang,[1†] Qinggang Li,[2†] Lige Zhang,[1] Jie Cui,[1] Hao Yu,[1] Xiaoyu Wang,[1] Xingyu Ouyang,[1] Fei Tao,[1] Ping Xu [1] and Hongzhi Tang [1*]

[1]*State Key Laboratory of Microbial Metabolism, and School of Life Sciences & Biotechnology, Shanghai Jiao Tong University, Shanghai, 200240, China.*

[2]*College of Biotechnology, Tianjin University of Science and Technology, Tianjin, 300457, China.*

Summary

Polycyclic aromatic hydrocarbons (PAHs) and dioxin-like compounds, including sulfur, nitrogen and oxygen heterocycles, are widespread and toxic environmental pollutants. A wide variety of microorganisms capable of growing with aromatic polycyclic compounds are essential for bioremediation of the contaminated sites and the Earth's carbon cycle. Here, cells of *Pseudomonas putida* B6-2 (ATCC BAA-2545) grown in the presence of biphenyl (BP) are able to simultaneously degrade PAHs and their derivatives, even when they are present as mixtures, and tolerate high concentrations of extremely toxic solvents. Genetic analysis of the 6.37 Mb genome of strain B6-2 reveals coexistence of gene clusters responsible for central catabolic systems of aromatic compounds and for solvent tolerance. We used functional transcriptomics and proteomics to identify the candidate genes associated with catabolism of BP and a mixture of BP, dibenzofuran, dibenzothiophene and carbazole. Moreover, we observed dynamic changes in transcriptional levels with BP, including in metabolic pathways of aromatic compounds, chemotaxis, efflux pumps and transporters potentially involved in adaptation to PAHs. This study on the highly versatile activities of strain B6-2 suggests it to be a potentially useful model for bioremediation of polluted sites and for investigation of biochemical, genetic and evolutionary aspects of *Pseudomonas*.

Received 7 April, 2021; revised 26 May, 2021; accepted 26 May, 2021. *For correspondence. E-mail tanghongzhi@sjtu.edu.cn; Tel. (+86) 21 34204066; Fax (+86) 21 34206723. †These authors contributed equally to the development of the work.

Introduction

Polycyclic aromatic hydrocarbons (PAHs) are persistent organic pollutants, found in wastes of coal tar, petroleum sludge, creosote and wood preservative. Sixteen PAHs with two to six rings have been identified as priority pollutants by the United States Environmental Protection Agency (EPA) (Keith and Telliard, 1979; Habe and Omori, 2003). Some PAHs are substituted by sulfur (S), nitrogen (N) and/or oxygen (O) atoms to form heterocycles such as dibenzothiophene (DBT), benzothiophene (BT), carbazole (CA), dibenzofuran (DBF), dibenzo-*p*-dioxin (DD) and diphenyl ether (DE) (abbreviations list in Table S1). Polychlorinated DDs and DBFs (PCDDs and PCDFs, respectively) are components of dioxin-like compounds (dioxins), together with waste industrial products polychlorinated biphenyls (PCBs) and polybrominated DEs (PBDEs) (Wittich, 1998). S, N, O heterocycles, PAHs and dioxins are toxic, mutagenic and carcinogenic environmental pollutants (Keith and Telliard, 1979; Kropp and Fedorak, 1998; Schecter *et al*., 2006; Perera *et al*., 2009). They are widespread around the world and they even coexist for months to years in the environment, eliciting serious health risks in many places (Blumenstock *et al*., 2000; Gullett *et al*., 2003).

Microorganisms play important roles in natural degradation of S, N, O heterocycles, PAHs and dioxins (Xu *et al*., 2006; Chang, 2008; Ghosal *et al*., 2016; Lu *et al*., 2011), and therefore are essential for processes of bioremediation of contaminated sites and for transitioning the Earth's carbon cycle between organic and inorganic states. Many microorganisms capable of growing with aromatic polycycles have been isolated, and *Pseudomonas* is the dominant isolated genus (Grifoll *et al*., 1995; Eaton and Nitterauer, 1994; Nojiri *et al*., 1999; Li *et al*., 2006; Ma *et al*., 2006). Other genera include *Sphingomonas* (Gai *et al*., 2007), *Terrabacter* (Habe

et al., 2002), *Janibacter* (Yamazoe *et al*., 2004), *Ralstonia* (Schneider *et al*., 2000), *Burkholderia* (Camara *et al*., 2004) and *Beijerinckia* (Kim and Zylstra, 1995). Genetics of bacterial degradation pathways, especially biphenyl degradation and co-metabolism of PCBs, have been studied (Seeger and Pieper, 2010). However, toxic metabolites such as hydroxylated polycycles and ring-cleavage products have been frequently detected to accumulate as end products, leading to secondary pollution of the environment (Wittich, 1998; Grifoll *et al*., 1995; Camara *et al*., 2004; Waldau *et al*., 2009). Many structurally similar aromatic polycycles coexisting in the environment could be cometabolically attacked by microorganisms growing with other aromatic polycycles (van Herwijnen *et al*., 2003; Peng *et al*., 2008). *Mycobacterium* species can degrade a wide variety of PAHs, including low and high molecular weight PAHs, such as phenanthrene, fluoranthene, pyrene and benzo[***a***]pyrene (Dudhagara and Dave, 2018). Synergy and antagonism are two features of PAH mixture degradation, and metabolic competition can inhibit the degradation of PAH mixtures (Hennessee and Li, 2016).

Additionally, organic solvents in oils, creosotes and industrial wastes always coexist in many polluted sites. Organic solvents with log P_{ow} (the logarithm of the partition coefficient of a solvent in an octanol–water mixture) below 5.0 are extremely toxic for cells even at a low concentration of 0.1% (V/V) (Isken *et al*., 1999; Inoue and Horikoshi, 1989; Isken and de Bont, 1998). The functional bacteria in those sites have to fight against these solvents to survive before degrading aromatic polycycles. Functional genes have been transformed into solvent-tolerant bacteria to construct strains for industrial processes occurring in biphasic systems (Wierckx *et al*., 2005; Tao *et al*., 2006). Microbial-based remediation needs to overcome two major problems: mixed aromatic polycycles and extremely toxic organic solvents. It is, however, feasible to construct such strains for improvement of bioremediation processes.

In previous studies, we found a new pathway for mineralization of DBF by a naturally isolated *Pseudomonas putida* B6-2, and the draft genome sequence of *P. putida* B6-2 has been published (Tang *et al*., 2011). Moreover, strain B6-2 possesses two efflux pumps responsible for organic solvent tolerance and antibiotic resistance, and these two pumps are controlled by SrpR-mediated cross regulation (Li *et al*., 2009; Tang *et al*., 2011; Yao *et al*., 2017; Yao *et al*., 2020). Here, the abilities of strain B6-2 to deal with mixed aromatic polycycles and survive in extremely toxic organic solvents were tested. We also found that strain B6-2 integrates a wide range of aromatic catabolic pathways, including biphenyl, benzoate, 4-hydroxybenzoate, salicylate and catechol. This integration should be an advantage of strain B6-2 in degrading aromatic compounds and their derivatives.

Multi-omics have been previously applied to discover novel pathways in environmental bacteria. Based on the analysis of whole genome and proteomic data, the novel upstream pathway of nicotine degradation was uncovered in *P. putida* S16 (Tang *et al*., 2013). Two possible gene clusters of indole degradation were identified by genomic and proteomic analysis in *Cupriavidus* sp. strain SHE (Qu *et al*., 2017). In *Methylobacterium* sp. strain DM1, whole-genome sequencing was performed to infer *N*,*N*-dimethylformamide (DMF) degradation pathway, and RNA-seq was used to identify the novel gene clusters (including DMF degradation, dimethylamine degradation, methylamine degradation and formate metabolism) in response to DMF (Lu *et al*., 2019).

In order to provide information on the genetics of metabolic capacity and environmental behaviours, we sequenced the whole genome of strain B6-2 and performed the genetic analysis of aromatic chemical catabolism in the potential microbe for bioremediation of PAH pollution. We further analysed profiles of gene transcription and protein expression during incubation of the bacterium with BP and a mixture of BP/CA/DBF/DBT using complete genomic analysis, a high-throughput whole-cell proteome and transcriptome analysis. Analysis of the multi-omics data illustrates the genetic characteristics of *P. putida* and points to potential applications in bioremediation of PAH pollution and production of fine chemicals.

Results

Degradation of individual PAHs and identification of metabolites

The range of aromatic compounds as substrates of strain B6-2 was investigated; benzoate was detected as a metabolite of BP (Table S2) and capable of supporting strain B6-2 cell growth. In addition, CA, salicylate, 4-hydroxybenzoate and catechol supported the growth of strain B6-2, whereas fluorene (FN), DBT, BT, diphenyl either (DE) and dibenzo-*p*-dioxin (DD) did not (Table S3). BP-grown B6-2 cells were able to degrade all individual tested compounds including FN, CA, DBT, BT, DD, DE, 4,4′-dichlorobiphenyl (4,4′-DCBP), 2,2′-dichlorobiphenyl (2,2′-DCBP), 4-bromodiphenyl ether (4-BDE) and 2-chlorodibenzo-p-dioxin (2-CDD), respectively (Fig. 1A–H, Table S2).

Co-metabolism of FN and CA. 9-Fluorenol (FN1) and 9-fluorenone (FN2) were detected as the major metabolites of FN catabolism using high-performance liquid chromatography (HPLC) (Fig. 1B). In addition, 2-hydroxy-

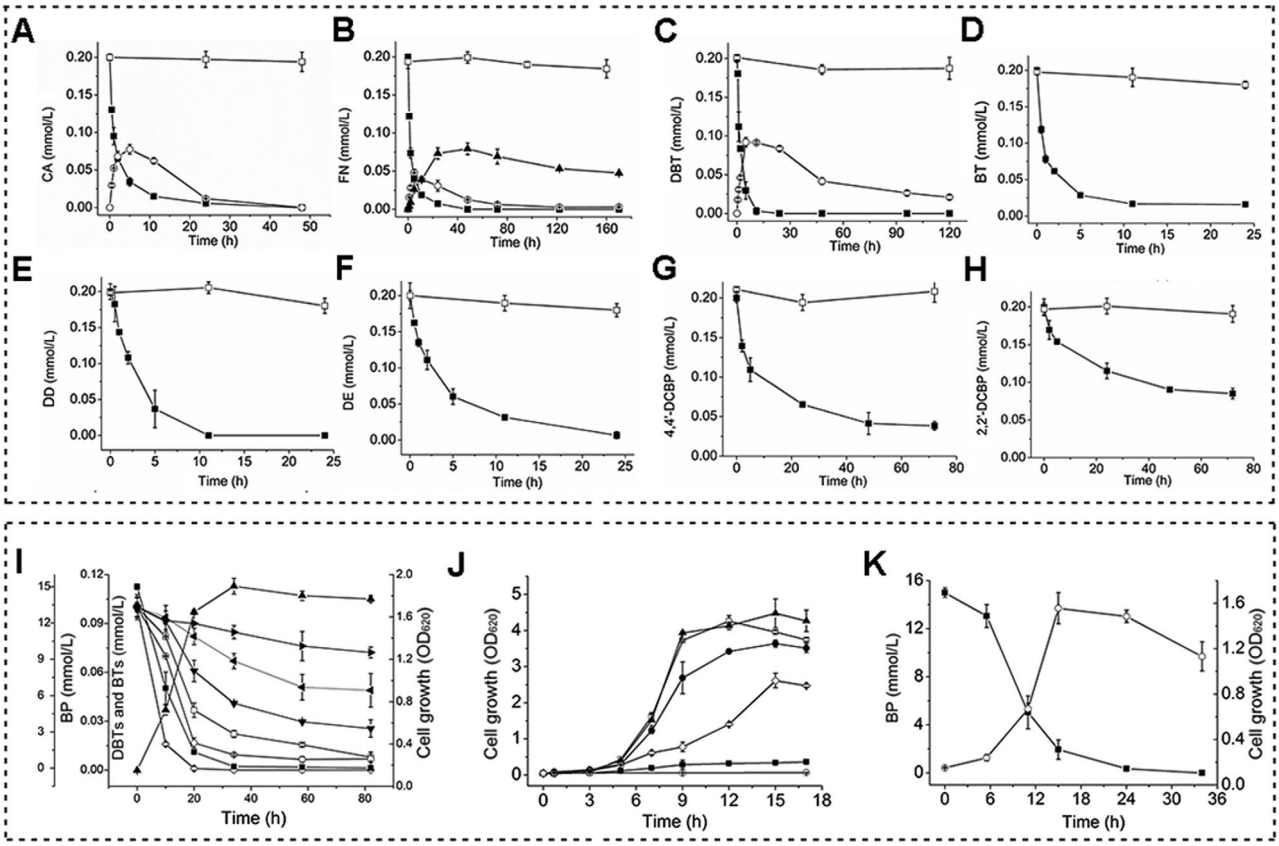

Fig 1. Degradation of various aromatic substrates and production of major metabolites by BP-grown cells of *P. putida* strain B6-2.
A. CA (■) and 3-hydroxycarbazole (CA1, ○).
B. FN (■), 9-fluorenol (FN1, ○) and 9-fluorenone (FN2, ▲).
C. DBT (■) and 2-hydroxy-4-(3′-oxobenzothiophene-2′-ylidene)but-2-enoic acid (DBT1, ○).
D. BT (■).
E. DD (■).
F. DE (■).
G. 4,4′-DCBP (■).
H. 2,2′-DCBP (■).
In every test, autoclaved incubations with substrates served as controls (□). Degradation of sulfur-containing aromatic compounds by strain B6-2 and tolerance of organic solvents.
I. B6-2 Cell growth (▲) with 15 mmol l^{-1} BP (■) and concomitant degradation of 0.1 mmol l^{-1} of 4,6-DMDBT (►), 4-MDBT (◄), DBT (▼), BT (□), 2-MBT (○) and 5-MBT (◊).
J. B6-2 cell growth in LB medium (□) and in LB medium plus 20% (V/V) of *n*-decane (▲), *n*-heptane (●), *p*-xylene (◊), toluene (■) or benzene (○).
K. B6-2 cell growth (○) with BP (■) in MSM plus 0.5% (V/V) *p*-xylene.

4-(1′-oxoinden-2′-ylidene)but-2-enoic acid (FN5) with absorption maximum of 462 nm was identical to the meta-cleavage product of 3,4-dihydroxyfluorene (Grifoll *et al*., 1995). Other metabolites like 1-indanone (FN3) and benzo[c]chromen-6-one (FN4) were detected and identified from FN catabolism culture by gas chromatography–mass spectrometry (GC–MS). 3-Hydroxycarbazole (CA1) was detected as the major metabolite of CA (Fig. 1A). Isatin (CA4), anthranilate (CA5), 4-quinolinone (CA6) and 3-(2-aminophenyl)-3-oxopropanoic acid (CA7) were detected during CA degradation.

Co-metabolism of DBT and BT. 2-Hydroxy-4-[3′-oxobenzothiophene-2′-ylidene]but-2-enoic acid (DBT1) was detected as the major metabolite of DBT (Fig. 1C). Other metabolites, hydroxydibenzothiophene (DBT2), DBT-S-oxide (DBT3), BT-2,3-dione (DBT4) and 2-mercaptobenzoate (DBT5) were detected as the minor metabolites of DBT (Table S2). In addition, compounds BT-S-oxide (BT1), BT-S,S-dioxide (BT2), DBT4 and DBT5 were formed from BT catabolism.

Co-metabolism of DD, DE and BDE. The DD degradation product DD1M has a molecular ion at m/z 276. This

fragmentation pattern is typical for methylated lateral dioxygenation and meta-cleavage products of acenaphthylene, DBF and CA. Therefore, DD1M is suggested to be 4-(3-hydroxybenzo[*b*][1,4]dioxin-2-yl)-2-oxo-3-butenoic acid, a ring-cleavage product involved in DD 1,2-dioxygenation and the *meta*-cleavage pathway. The DE degradation product DE1 should be a mono-hydroxylated DE. The 4-BDE degradation product 4-BDE1 is proposed to be 4-bromophenol.

Co-metabolism of 2-CDD, 4,4′-DCBP and 2,2′-DCBP. 2-CDD1M was detected from 2-CDD degradation sample. It has a molecular mass of 158. Accordingly, it is proposed to be monomethylated 3-chlorocatechol. 4,4′-CB1M was detected from 4,4′-DCBP degradation sample using GC–MS. It has a molecular ion at m/z 170, indicating the presence of a methylated carboxyl group and Cl atom in the molecule. Accordingly, it is proposed to be monomethylated 4-chlorobenzoate. 2,2′-CB1M was detected from the 2,2′-DCBP degradation sample. It has a similar MS profile with that of 4,4′-CB1M and is suggested to be monomethylated 2-chlorobenzoate.

Degradation of mixed aromatic compounds and tolerance of solvents

Thirteen of 16 standard EPA-PAHs including FN, phenanthrene, anthracene, fluoranthene, pyrene, benzo[*a*] anthracene, chrysene, benzo[*b*]fluoranthene, benzo[*k*] fluoranthene, benzo[*a*]pyrene, dibenzo[*a*,*h*]anthracene, benzo[*g*,*h*,*i*]perylene and indeno[1,2,3-*cd*]pyrene were identified from an extract of PAH-contaminated soil (see methods for details). Degradation of the extract by BP-grown B6-2 cells was detected. After a 120-h incubation, all of these PAHs were significantly degraded (48.8% to 76.8%, 100% for FN and anthracene, respectively) based on comparing their concentrations in the sample and the control culture (Table 1).

BP-grown B6-2 cells also showed extensive degradation ability towards the seven tested dioxins including 2,8-DCDF, 2-CDD, 4-BDE, 4,4′-dibromodiphenyl ether (4,4′-DBDE), 3,4-dichlorobiphenyl (3,4-DCBP), 4,4′-DCBP and 2,2′-DCBP (Table 2). After a 12-h incubation, most of the compounds decreased to about half of their original amounts. After a 72-h incubation, 69.6% to 90.8% of the original compounds were degraded, respectively.

B6-2 cells grown with BP as a primary substrate simultaneously degraded each compound in a mixture including DBT, 4-MDBT, 4,6-dimethyldibenzothiophene (4,6-DMDBT), BT, 2-methylbenzothiophene (2-MBT) and 5-methylbenzothiophene (5-MBT) (Fig. 1I). The cell growth and concentrations of substrates were monitored. The optical density at 620 nm (OD_{620}) of the culture increased from 0.13 to a maximum of 1.89 within 34 h. After an 82-h incubation, 100% of BP and 5-MBT, 99% of 2-MBT and BT, 75% of DBT, 51% of 4-MDBT and 28% of 4,6-DMDBT were degraded.

After preincubation in LB medium exposed to 0.3% *p*-xylene (log P_{ow} 3.1), strain B6-2 grew well in LB medium plus 20% of *n*-decane (log P_{ow} 5.6), *n*-heptane (log P_{ow} 4.1), or *p*-xylene. Only slight growth was detected when 20% toluene (log P_{ow} 2.5) was added, and almost no growth was detected when 20% benzene (log P_{ow} 2) was added (Fig. 1J). When the volume ratio of organic solvents (*n*-decane, *n*-heptane, *p*-xylene and toluene) was increased from 20% to 100%, growth of the strain was not significantly inhibited only in *n*-decane (Fig. S1). In addition, B6-2 cells grew well in MSM with BP under the stress of 0.5% *p*-xylene (Fig. 1K). Genome sequencing and similarity search results reveal two efflux pump systems, toluene tolerance genes (Ttg)ABC and solvent resistant pump (Srp)ABC, in strain B6-2. The similarity

Table 1. Degradation of 13 EPA-PAHs by BP-grown cells of *P. putida* B6-2.

Substrate	Concentration of substrate at day 5 (nmol l^{-1})		Remove (%)
	Control	Sample	
Fluorene	175.3 ± 7.8	0	100
Phenanthrene	1145.5 ± 79.2	410.1 ± 70.8	64.2 ± 6.2
Anthracene	108.4 ± 8.4	0	100
Fluoranthene	2632.7 ± 18.3	935.1 ± 62.4	64.5 ± 2.4
Pyrene	1772.8 ± 60.9	668.8 ± 31.2	62.3 ± 1.8
Benzo[*a*] anthracene	370.6 ± 3.5	156.1 ± 6.1	57.9 ± 1.7
Chrysene	1507.5 ± 0.4	546.9 ± 58.3	63.7 ± 3.9
Benzo[*b*] fluoranthene	1022.2 ± 1.59	323.0 ± 21.8	68.4 ± 2.2
Benzo[*k*] fluoranthene	625.8 ± 9.5	227.8 ± 14.7	63.6 ± 2.3
Benzo[*a*]pyrene	641.7 ± 58.3	328.2 ± 29.8	48.8 ± 4.7
Dibenzo[*a*,*h*] anthracene	235.6 ± 6.5	110.1 ± 3.2	53.3 ± 1.4
Benzo[*g*,*h*,*i*] perylene	1598.2 ± 38.0	371.4 ± 16.7	76.8 ± 1.1
Indeno[1,2,3-*cd*] pyrene	469.9 ± 8.3	218.5 ± 13.4	53.5 ± 2.9

Table 2. Degradation of seven dioxins by BP-grown cells of *P. putida* B6-2.

Compound	Remove (%)	
	After 12-h incubation	After 72-h incubation
2,8-DCDF	43.1 ± 2.2	90.8 ± 6.8
2-CDD	45.4 ± 7.4	82.7 ± 4.0
4-BDE	44.4 ± 1.5	89.9 ± 2.8
4,4′-DBDE	31.8 ± 3.4	72.3 ± 4.8
3,4-DCBP	50.1 ± 2.2	84.7 ± 1.7
4,4′-DCBP	45.4 ± 3.6	78.9 ± 3.4
2,2′-DCBP	21.6 ± 3.1	64.6 ± 4.8

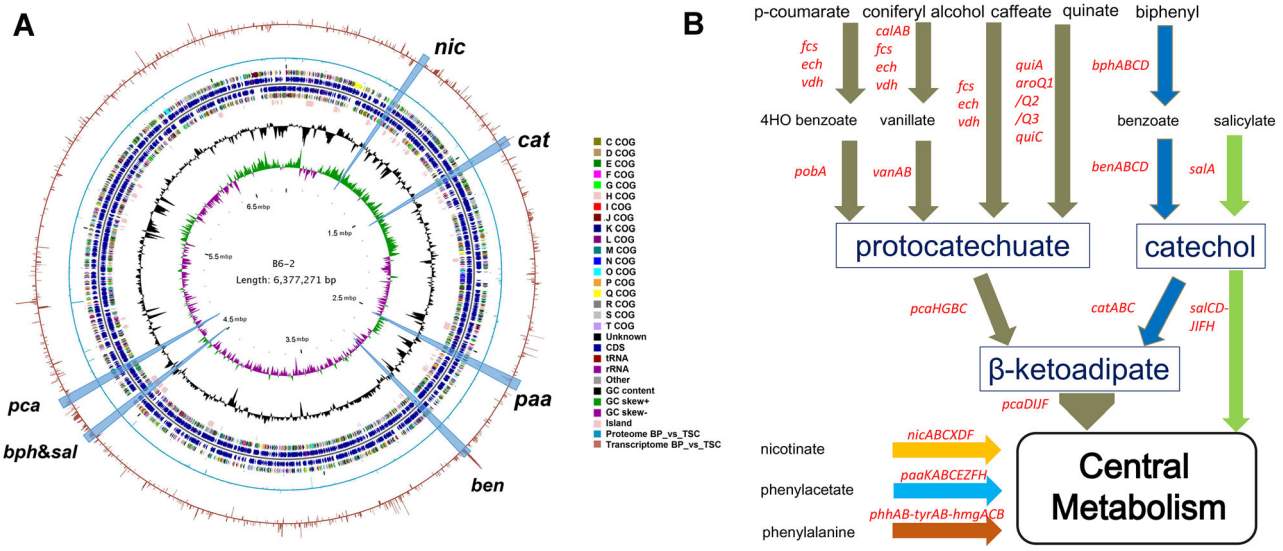

Fig 2. Schematic representation of the *P. putida* B6-2 genome.
A. The circles represent (from the inside inwards): Circle 1, the scale, spaced every 200 kbp; Circle 2, G + C skew (purple <0 ≤ green); Circle 3, % G + C content; Circle 4, genomic islands predicted in the B6-2 chromosome; Circles 5 and 6, the COG function classification and (clockwise) locations of CDs, tRNA and rRNA, respectively; Circles 7 and 8, the COG classification and (anti-clockwise) locations of CDs, tRNA and rRNA, respectively. The COG categories are as the legend in Fig. 3. Circles 9 and 10, proteome and transcriptome information of differentially expressed genes in biphenyl medium and trisodium citrate medium ($|\log_2 FC| > 1$, $\log_2$ (FC) = $\log_2$ (RNA mean (Group BP/Group TSC). The location of six gene clusters encoding the aromatic metabolic pathways were predicted on B6-2 complete genome (the blue arrow), *nic* (the nicotinate pathway), *cat* (the catechol pathway), *paa* (the phenylacetate pathway), ben (the benzoate pathway), *bph&sal* (the biphenyl and salicylate pathways), *pca* (the protocatechuate pathway).
B. Aromatic compounds catabolic pathways predicted in *P. putida* B6-2. The central aromatic catabolic pathways are presented below: The β-ketoadipate pathway is composed of two branches, the protocatechuate branch (including *p*-coumarate, conifeyl alcohol, cafffeate, quinate, 4-hydroxybenzoate and vanillate) and the catechol branch (including biphenyl, benzoate and salicylate); the phenyl acetyl-coA pathway; the homogentisate pathway; the nicotinate pathway.

between *srpABC* and its counterpart in *P. putida* strain S12 is almost 100% (with a difference of only two bases), and *ttgABC* shares over 99.0% identity to its counterpart in *P. putida* DOT-T1E (Kieboom *et al*., 1998). TtgABC and SrpABC were demonstrated to be involved in the solvent tolerance of strain B6-2 in our previous study (Yao *et al*., 2017).

Genome anatomy

The draft genome sequence of strain B6-2 was determined and the reads were assembled into 27 large contigs (Tang *et al*., 2011). In order to further locate the gene clusters of PAH metabolic pathways and understand the characteristics of the oxidoreductase system in strain B6-2, we sequenced the complete genome of B6-2 (Fig. 2A, GenBank: CP015202.1). The features for the complete genome sequence of *P. putida* B6-2 are summarized in Table S4.

According to the results of Rapid Annotations using Subsystems Technology (RAST), we found 537 subsystems, and 5832 coding sequences including 181 genes (3.1%) related to metabolism of aromatic compounds, such as salicylate, biphenyl, benzoate, *p*-hydroxybenzoate and chloroaromatics. The genes involved in aromatic catabolic pathways, such as the biodegradation pathways of protocatechuate, catechol, salicylate, nicotinate, phenylacetate and phenylalanine, are predicted to colocalize on the chromosome of B6-2 genome (Fig. 2B). Additionally, 32 genes encoding dioxygenases were found in the genome annotation of strain B6-2. Various genes related to metabolism of aromatic compounds and dioxygenases were found in the B6-2 genome sequence, and are the reason why strain B6-2 can efficiently degrade PAHs. Moreover, 120 genes related to motility and chemotaxis were found in the B6-2 genome, including at least five clusters of chemotaxis genes (Table S5). Chemotaxis may enhance the motility of bacteria to locate and degrade chemical compounds (Sampedro *et al*., 2014). These gene clusters will further inform characterization of the PAH degradation ability in strain B6-2.

The genome contains diverse mobile element protein-coding genes, including 80 mobile element sequences, 20 integrases and 3 retrons, including near the biphenyl and salicylate metabolism gene cluster (Table S6). The region of B6-2 genome at positions 4,544,583 to 4,667,612 (123,029 bp) was predicted to be one genomic island, and this region contains *bph* and *sal* gene clusters (Fig. S2). Clusters of horizontally acquired genes, or genomic islands, are frequently associated with particular

physiologic adaptations such as virulence, catabolism, or resistance to a toxic compound.

Proteomic profiling of strain B6-2

A proteomic analysis comparing the treatment group (with BP or mixed BP/CA/DBF/DBT as the sole carbon source) with the control group (with trisodium citrate as the sole carbon source) was performed to identify functional genes involved in BP metabolism. A total of 3441 proteins were identified, accounting for 59.0% of the genomic CDSs in strain B6-2. After global normalization and *t*-test analysis, 956 proteins have significant changes in expression (≥2-fold changes, $p < 0.05$) in response to BP metabolism: 395 proteins are up-regulated and 561 proteins are down-regulated (Fig. 3A). When using the mixed BP/CA/DBF/DBT as a carbon source, 397 proteins are up-regulated and 551 proteins are down-regulated (Fig. 3B). After comparing the two treatment (MIX to BP) groups, 33 proteins were found to be up-regulated and 43 proteins were down-regulated (Fig. 3C). According to gene annotations, BP metabolism-related

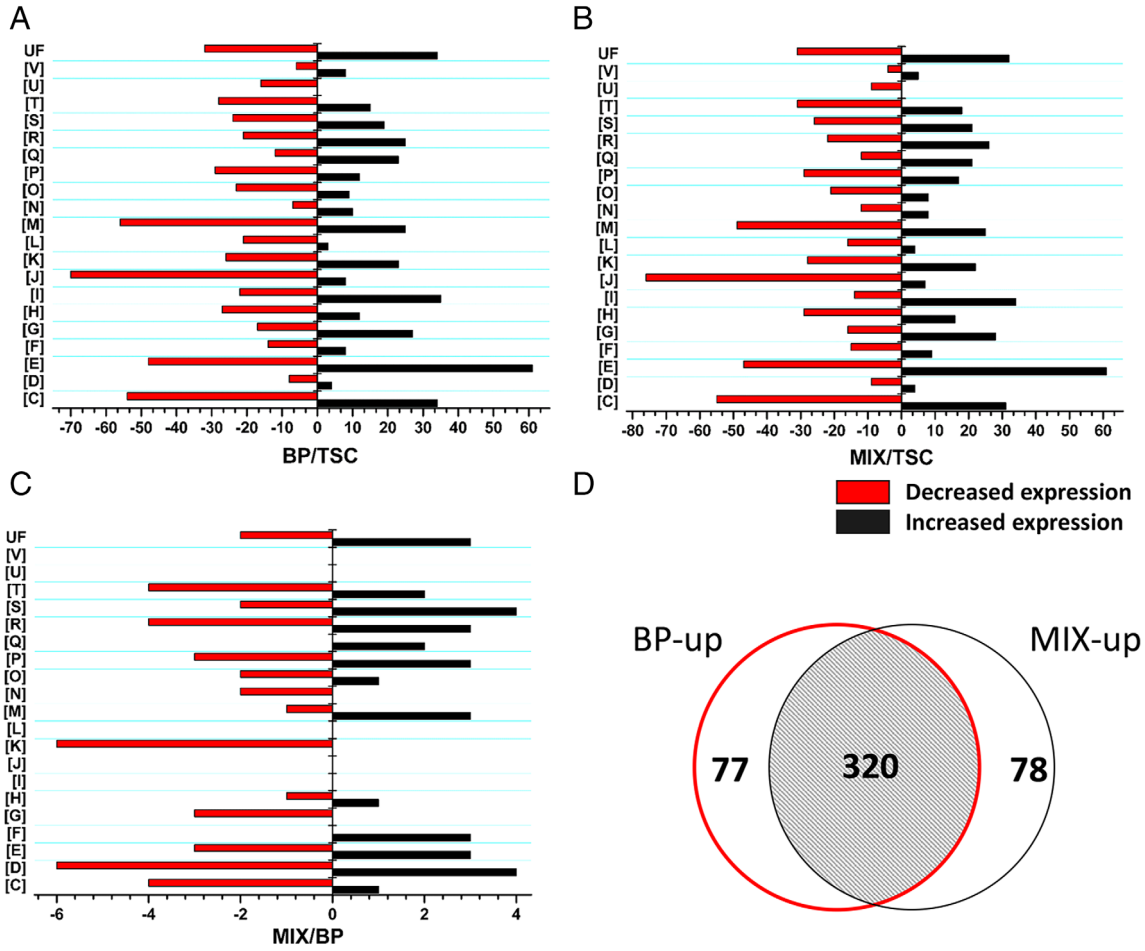

Fig 3. Cluster analysis of differently expressed proteins of strain B6-2 in BP, mixed carbon source BP/CA/DBF/DBT (MIX) and trisodium citrate (TSC) medium. COG categories of up-regulated and down-regulated proteins identified from strain B6-2 cells grown in the medium with or without biphenyl based on the proteome analysis. 'Increased expression' means proteins were >2-fold up-regulated in biphenyl medium compared with the control; 'decreased expression' means proteins were >2-fold down-regulated.
A. Cluster analysis of differently expressed proteins in BP and TSC medium.
B. Cluster analysis of differently expressed proteins in MIX and TSC medium.
C. Cluster analysis of differently expressed proteins in MIX and BP medium.
D. Venn diagram of up-regulated proteins response to BP (BP-up) and up-regulated proteins response to MIX (MIX-up).
COG codes: [C] Energy production and conversion; [D] Cell cycle control, cell division, chromosome partitioning; [E] Amino acid transport and metabolism; [F] Nucleotide transport and metabolism; [G] Carbohydrate transport and metabolism; [H] Coenzyme transport and metabolism; [I] Lipid transport and metabolism; [J] Translation, ribosomal structure and biogenesis; [K] Transcription; [L] Replication, recombination and repair; [M] Cell wall/membrane/envelope biogenesis; [N] Cell motility; [O] Posttranslational modification, protein turnover, chaperones; [P] Inorganic ion transport and metabolism; [Q] Secondary metabolites biosynthesis, transport and catabolism; [R] General function prediction only; [S] Function unknown; [T] Signal transduction mechanisms; [U] Intracellular trafficking, secretion and vesicular transport.

genes are mainly located in clusters of energy production and conversion, secondary metabolite catabolism and general function with increased expression. In addition, 320 proteins in both BP medium and MIX medium are up-regulated (Fig. 3D).

The proteomic data were further analysed, and the numbers of up-regulated proteins belonging to categories E (amino acid transport and metabolism), I (lipid transport and metabolism) and C (energy production and conversion) are higher than proteins in other categories. More up-regulated proteins were identified in I (lipid transport and metabolism) than down-regulated proteins, and more down-regulated proteins were identified in J (translation, ribosomal structure and biogenesis) than up-regulated proteins. Eighteen genes related to dehydrogenases have increased expression in the up-regulated proteins, indicating that there may be a need for up-regulation of proteins associated with PAH cometabolism. Approximately 9 outer membrane proteins (OMP), 5 chemotaxis proteins and cold shock domain protein (CspD) are up-regulated in strain B6-2; these proteins may play important roles in sensing PAHs.

Also, 42 proteins were expressed with intensities at least fivefold higher in BP-grown B6-2 cells versus those in sodium citrate-grown cells according to the 2-D gel electrophoresis analytical results (Fig. S3). Twenty-eight of these proteins were identified and subsequent searching through the SWISS-PROT and NCBInr databases, and in silico databases (Table S7). Seventeen proteins have their counterparts in strains LB400 and *P. putida* F1, KT2440, GB-1 and W619, which are probably involved in aromatic compound catabolism. These 17 proteins were functionally clustered into three parts including BP-degrading enzymes, benzoate-degrading enzymes, and some putative dioxygenases, dehydrogenases, reductases and hydratases/isomerases.

Transcriptomic analysis of aromatic compound catabolism

In order to identify the differently expressed genes (DEGs) of strain B6-2 in response to biphenyl, the transcriptomic analysis was performed. We identified 686 genes that are up-regulated, and 333 genes that are down-regulated in the biphenyl cultured group (Fig. 4A). As shown in Fig. 4B, the cluster analysis of DEGs reveals obvious correlations in the same group response to biphenyl or trisodium citrate. Genes with similar expression patterns are classified into the same category, in order to find unknown biological functions of genes through cluster analysis. To reveal the catabolic response involved in biphenyl degradation, we investigated transcriptome data related to the metabolism of aromatic compounds. According to the RAST database, aromatic metabolism-related genes of strain B6-2 were classified into 16 subsystems and 181 genes were postulated to be involved in metabolism of aromatic compounds. Among them, we found that genes belonging to the subsystems 'biphenyl degradation', 'benzoate degradation', 'catechol branch of beta-ketoadipate pathway' and 'central meta-cleavage pathway of aromatic compound degradation' were significantly upregulated when cultured in biphenyl medium (Fig. 4C). According to KEGG pathway enrichment analysis, DEGs are mainly enriched in two-component system, oxidative phosphorylation and benzoate degradation pathways (Fig. 4D).

Multi-omics analysis for catabolism of BP, benzoate, 4-hydroxybenzoate and salicylate

By combining genomic, proteomic and transcriptomic data of strain B6-2, the gene clusters that encode the enzymes for catabolism of BP, benzoate, 4-hydroxybenzoate and salicylate were obtained (Fig. 5). At least five enzymes in B6-2 could catalyse catechol ring cleavage (*pcaG-H*, *bphC*, *catA1*, *catA2* and *salC*). Figure 5B shows the *bph* gene cluster encoding BP upper degradation enzymes (*bphR-bphA1A2-orfx-bphA3A4BC*) and the lower enzymes (*bphKHJID*) for 2-hydroxypenta-2,-4-dienoate degradation. Transcription levels of the *bph* genes are significantly up-regulated, including the GntR family regulator related-gene *bphR1* (fold-change from 3.0 to 5.8, $p < 0.01$; see Table S8 for details). In addition, the *bph* genes, *bphA1A2A3A4BCKHJID*, are significantly overexpressed in the presence of BP and MIX (BP, CA, DBT and DBF) according to the proteomic data (fold-change from 3.8 to 7.5, 2.8 to 8.9, respectively; $p < 0.01$).

Genes encoding enzymes for transforming benzoate to *cis*,*cis*-muconate through catechol 1,2-dioxygenation are shown in Fig. 5C. Figure 5D shows another catechol degradation pathway. *Cis*,*cis*-muconate, in cooperation with the positive transcription regulator CatR, can activate the expression of enzymes CatA1 (catechol 1,2-dioxygenase), CatB (muconolactone isomerase) and CatC (muconate cycloisomerase) that transform catechol to β-ketoadipate enol-lactone (Jiménez *et al*., 2014). CatA1 and CatB are among the most up-regulated proteins (363.0-fold and 2768.9-fold, respectively; $p < 0.01$), providing evidence that the cluster *catA1BC* is the main metabolic pathway of catechol. In addition, transcription levels of the *catA1BC* genes are significantly up-regulated in response to biphenyl with 148.7-fold, 30.7-fold and 118.4-fold ($p < 0.01$) (Table S8).

β-Ketoadipate enol-lactone can also be produced from 4-hydroxybenzoate through a protocatechuate ortho-cleavage pathway by enzymes 4HbA (*pobA*) (4-hydroxybenzoate hydroxylase), 4-HbB (*pcaGH*) (protocatechuate 3,4-dioxygenase), 4-HbC (*pcaB*) (3-carboxy-*cis*,*cis*-muconate

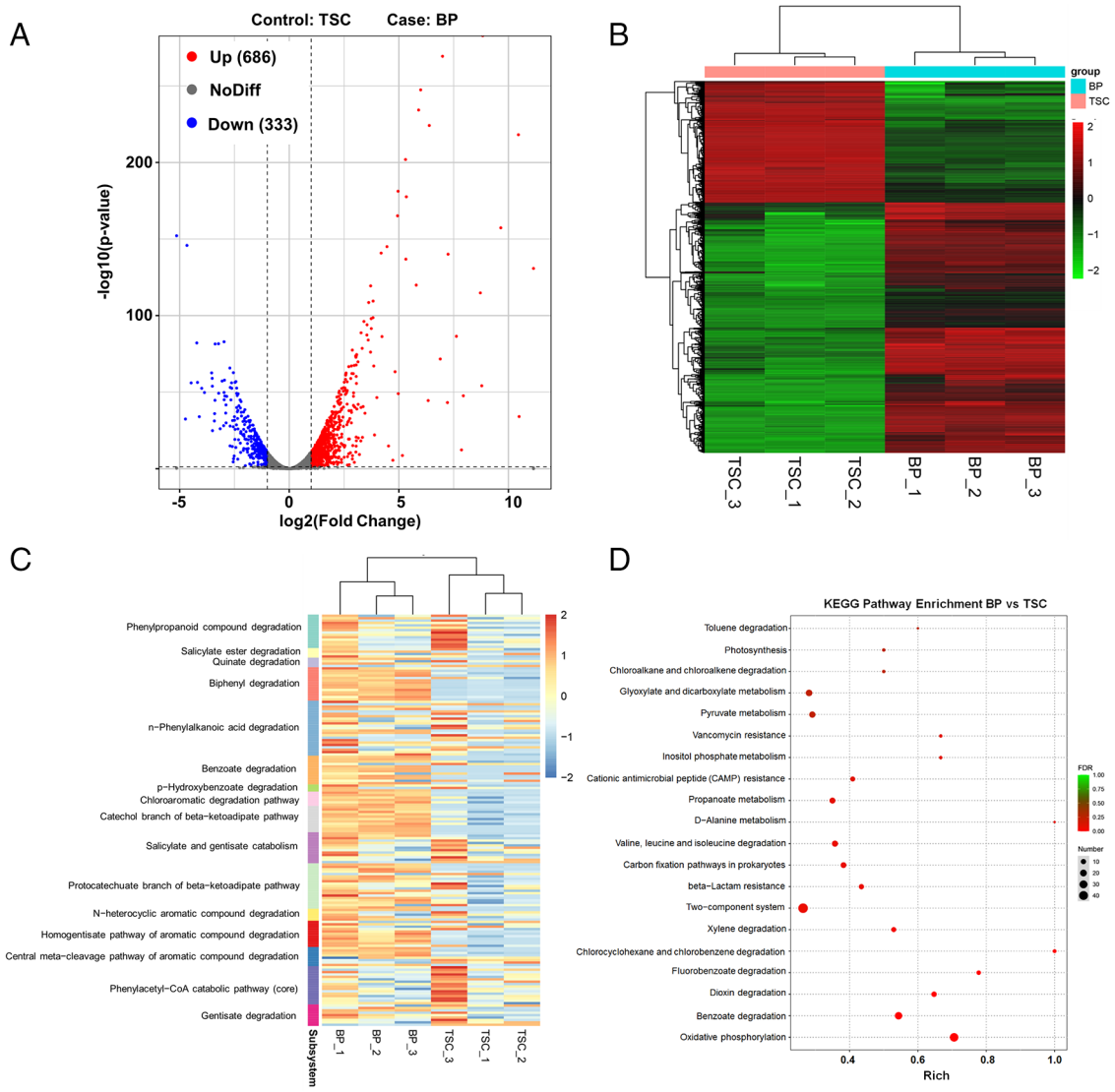

Fig 4. Analysis of transcriptome data.
A. Volcano map of different expressed genes (DEGs) in response to biphenyl. The red dots represent the up-regulated genes (686), the blue dots represent the down-regulated genes (333) and the grey dots represent the gene expression with no significant difference. The horizontal dashed line is the threshold of p-value = 0.05; the two vertical dotted lines are thresholds of $|\log_2 FC| > 2$.
B. Heat map presentation of the 1019 differentially expressed genes, including 686 up-regulated genes and 333 down-regulated genes [$|\log_2 FC| > 2$, $\log_2$ (FC) = $\log_2$ (RNA mean (Group BP/Group TSC))] involved in biphenyl degradation.
C. Sub heat map of 'metabolism of aromatic compounds (based on RAST annotation)' related genes involved in biphenyl degradation based on the transcriptome data.
D. KEGG pathway enrichment analysis of DEGs in response to biphenyl. The most significant enrichment of the top 20 KEGG pathways were displayed.

cycloisomerase) and 4-HbD (*pcaC*) (4-carboxy-muconolactone decarboxylase) (Fig. 5A). β-Ketoadipate enol-lactone can be further transformed by β-ketoadipate enol-lactone hydrolase (*pcaD*) to β-ketoadipate, which can be subsequently transformed by β-ketoadipate CoA-transferase (*pcaIJ*) and β-ketoadipyl CoA thiolase (*pcaF*) and eventually enter into the TCA cycle. The expression levels of genes *pcaC*, *pcpD*, *pcaI*, *pcaJ* and *pcaF* are relatively high at 11.8-fold ($p < 0.05$), 5.0-fold ($p < 0.01$), 195.4-fold ($p < 0.01$), 145.6-fold ($p < 0.01$) and 21.5-fold ($p < 0.01$), respectively. Moreover, transcription levels of the *pca*C/D/I/J/F genes are significantly up-regulated with fold-change from 2.7 to 10.2 ($p < 0.01$). The 4-hydroxybenzoate degradation genes shown in Fig. 5A are clustered into four groups, which are dispersed in the B6-2 genome. High levels of transcription (59.8-fold, $p < 0.01$) and expression (2212.7-fold, $p < 0.01$) of 4-hydroxybenzoate hydroxylase encoding gene (*pobA*) in

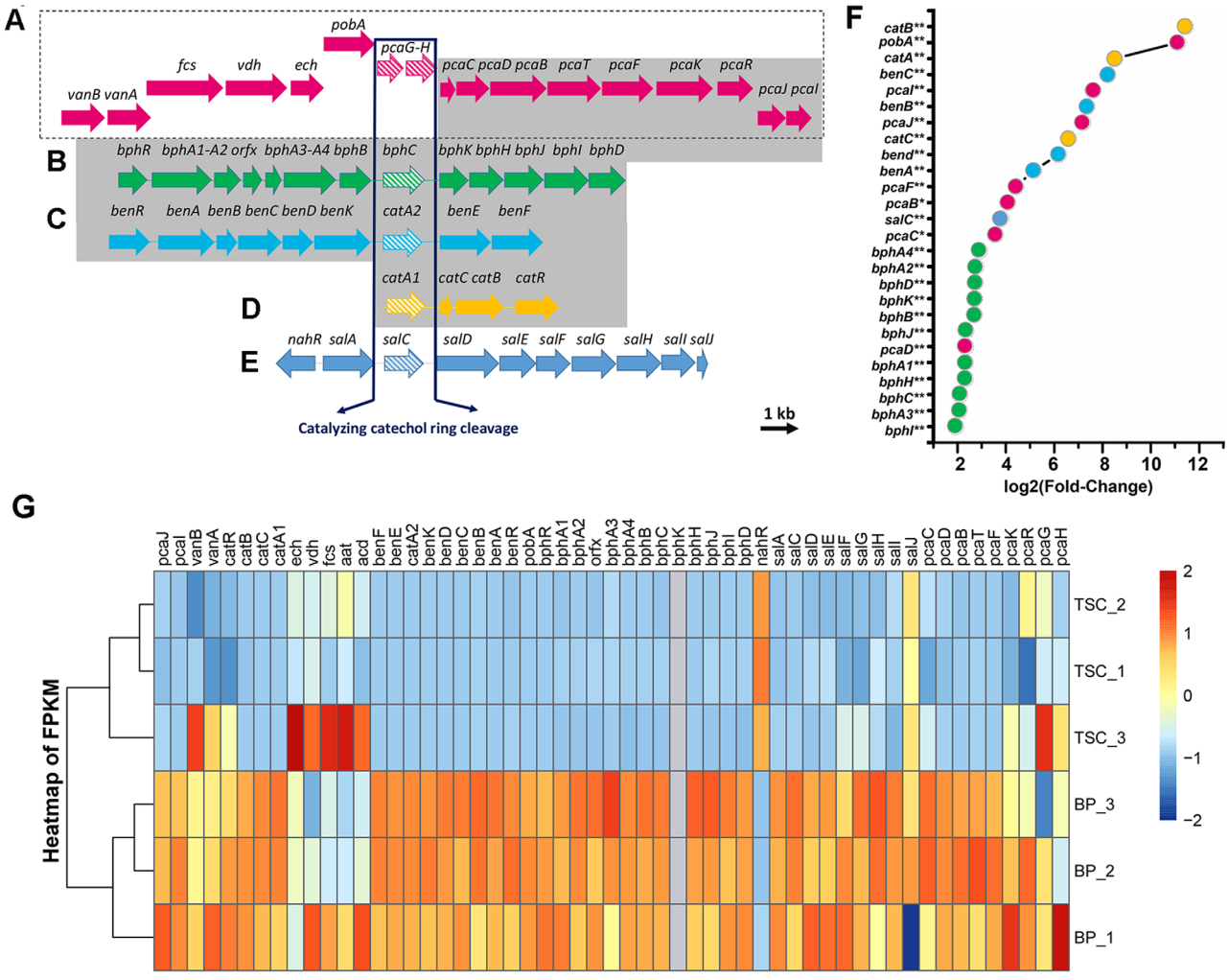

Fig 5. Genes in strain B6-2 for aromatic chemical catabolism. Genes responsible for utilizing BP as a sole source of carbon are shown in grey shading. Gene clusters encoding enzymes involved in benzoate (a metabolite of BP) mineralization are signed as BP lower pathway. Genes encoding dioxygenase capable of cleaving catechol are shown in the blue rectangle.

A. 4-Hydroxybenzoate degradation genes (in red arrow). Vanillate is converted to protocatechuate by the O-demethylase encoded by *vanAB*. Caffeate to protocatechuate and p-conmatate to 4-hydroxybenzoate depend on CoA-dependent nonβ-oxidative pathway encoded by *fcs-vdh-ech*. 4-Hydroxybenzoate hydroxylase encoded by *pobA* convert 4-hydroxybenzoate to protocatechuate. Genes *pcaGH* encode protocatechuate 3,4-dioxygenase alpha and beta chain; *pcaC* encodes 4-carboxymuconolactone decarboxylase; *pcaD* encodes beta-ketoadipate enol-lactone hydrolase; *pcaB* encodes 3-carboxy-*cis*,*cis*-muconate cycloisomerase; *pcaT* encodes dicarboxylic acid transporter; *pcaF* encodes β-ketoadipyl CoA thiolase; *pcaK* encodes 4-hydroxybenzoate transporter; *pcaR* encodes β-ketoadipate pathway transcriptional regulators; *pcaIJ* encode β-ketoadipate CoA-transferase alpha and beta subunits.

B. BP degradation gene cluster (in green arrow) for upper pathway (*bphR-bphA1A2-orfx-bphA3A4BC*) and the lower 2-hydroxypenta-2,-4-dienoate pathway *(bphKHJID)*.

C. Benzoate degradation gene cluster in dark blue arrow. Gene *benR* encodes transcriptional activator; *benAB* encode benzoate 1,2-dioxygenase alpha and beta subunit; *benC* encodes ferredoxin reductase; *benD* encodes 1,2-dihydroxycyclohexa-3,5-diene-1-carboxylate dehydrogenase; *benK* encodes benzoate MFS transporter; *catA2* encodes catechol 1,2-dioxygenase; *benE* encodes benzoate transport protein; *benF* encodes benzoate specific porin.

D. Catechol β-ketoadipate pathway gene cluster in yellow arrow. Gene *catA1* encodes another catechol 1,2-dioxygenase; *catB* encodes muconolactone isomerase; *catC* encodes muconate cycloisomerase; *catR* encodes transcriptional regulator (LysR family).

E. A part of the salicylate degradation gene cluster in light blue arrow. Gene *nahR* encodes regulatory protein; *salA* encodes salicylate hydroxylase; *salC* encodes catechol 2,3 dioxygenase; *sal*D encodes 2-hydroxymuconate semialdehyde dehydrogenase; *salE* encodes 2-hydroxymuconic semialdehyde hydrolase; .*salF* encodes 2-oxopent-4-enoate hydratase; *salH* encodes 2-oxo-4-hydroxypentanoate Aldolase; *salI* encodes 4-oxalocrotonate decarboxylase; *salJ* encodes 4-oxalocrotonate isomerase.

F. Summary of the highly expressed genes related to biphenyl catabolism by proteomic analysis. Genes with up-regulation fold >2 were chosen. *t*-test was used to calculate statistical significance. Symbols: *, $p < 0.05$; **, $p < 0.01$.

G. Heat map of genes predicted to be involved in aromatic chemical catabolism according to transcriptomics analysis, including the degradation pathways of 4-hydroxybenzoate, biphenyl, benzoate, catechol and salicylate.

response to biphenyl catabolism were detected based on both transcriptome and proteome data.

There is also a salicylate-degrading gene cluster in strain B6-2 (Fig. 5E). Catechol in the salicylate metabolic pathway is catalysed by a catechol 2,3-dioxygenase (SalC). Catechol generated from salicylate or benzoate can therefore be degraded through both ortho- and meta-cleavage pathways. Transcription and expression levels of gene *salC* are significantly up-regulated (2.2-fold and 13.9-fold, respectively, $p < 0.01$). According to the analytical results and previous studies (Li *et al*., 2009; Denef *et al*., 2005; Fujihara *et al*., 2006; Harwood *et al*., 1994), we suggest that B6-2 is capable of transforming BP, benzoate, salicylate and 4-hydroxybenzoate via pathways.

BphA1 and substrate range of BphA

BphA1 is the α-subunit of biphenyl 2,3-dioxygenases (BphA), and it is the major determinant of substrate range. The BphA1 sequence of B6-2 shows high similarities with those of the model strains LB400 and KF707 (90.0% and 92.0%, respectively); the major difference is concentrated between the amino acid sites 234 and 377 (Fig. S4). Phylogenetic trees of naphthalene dioxygenases, dibenzofuran dioxygenases and biphenyl dioxygenases were inferred, and related sequences were divided into three types (Fig. S5). The structure of BphA1 (BphA1_model_B6-2) in stain B6-2 was determined by homology modelling. The structures obtained by homology modelling were docked with the PAHs small molecules, and the structure with the highest score was selected as the final docking result. Based on analysis of molecular docking, a series of interacting amino acids residues were identified: PHE 227, MET 231, HIS 233, VAL 234, HIS 239, ILE 287, LEU 330, PHE 375 (-Table S9 and Fig. S6A). The substrates, biphenyl, dibenzofuran, carbazole, dibenzothiophene, fluorine, diphenyl oxide and dibenzo-*p*-dioxin, were docked into the active site of BphA1, and the superposed structures of the mixtures are shown in Fig. S6B–I. Based on the docking analysis, the flexibility to various substrates of active site in BphA1 should be one reason why strain B6-2 has a wider substrate spectrum.

Discussion

Most previous studies focused on the abilities of bacteria to act on structurally similar polycycles, neglecting the issues of generation of toxic dead-end metabolites and the coexistence of other kinds of aromatic polycycles. In addition, the lateral dioxygenation was also catalysed by angular dioxygenases, but the laterally dioxygenated polycycles were not be further transformed (Nojiri *et al*., 1999; Yamazoe *et al*., 2004) because no dihydrodiol dehydrogenase gene was present in the gene clusters responsible for the angular dioxygenation and meta-cleavage pathways (Nojiri *et al*., 2001; Inoue *et al*., 2006; Iida *et al*., 2006). In this report, we show that strain B6-2 also has strong degradation abilities towards individual aromatic compounds including FN, CA, DBT, BT, DE, DD 4,4′-DCBP and 2,2′-DCBP (Fig. 1A–H). Versatility of strain B6-2 was demonstrated by analysing the metabolites of FN, CA, DBT, BT, DD, DE, 2-CDD, 4-BDE, 4,4′-DCBP and 2,2′-DCBP (Table S2). According to the analytical results, the catabolic pathways of FN, CA, DBT, BT, DD and DE by strain B6-2 are proposed in Fig. 6.

Identification of CA1 and CA2, which should be abiotic products of 3,4-dihydroxy-3,4-dihydrocarbazole (CA1R) and 1,2-dihydroxy-1,2-dihydrocarbazole (CA2R), respectively, indicates that strain B6-2 can catalyse 3,4- and 1,2-dioxygenation of CA (Waldau *et al*., 2009). The former product should be the main reaction because CA1 was detected as the major product of CA (Fig. 1A). CA4 was newly identified as a metabolite of CA and it is proposed to be a further degradation product of CA via the C3,4 lateral dioxygenation and *meta*-cleavage pathway compared with the generation of its analogue BT-2,-3-dione from DBT (Bressler and Fedorak, 2001). The ability of strain B6-2 to dioxygenate CA at the angular and lateral positions of C1,2 and C3,4 suggests that B6-2 is a versatile CA-degrading bacterium.

Identification of FN5 and FN3 from the FN degradation sample and DBT1, DBT2, DBT4 and DBT5 from the DBT degradation sample indicates that FN and DBT could also be degraded by strain B6-2 through the lateral dioxygenation and meta-cleavage pathways (Xu *et al*., 2006; Grifoll *et al*., 1995). Different from CA and DBT degradation, where the lateral dioxygenation pathways were the main routes (Fig. 1B and C), most of FN was monooxygenated at C9 to generate FN1. S oxygenation of DBT was also performed by B6-2 and DBT3 was detected as the corresponding product. FN1, FN2 and DBT3 have been detected as common cometabolic degradation products by several BP-utilizing strains. However, only a few of those strains could further transform FN2 (Waldau *et al*., 2009). BT degradation was initiated by oxygenation at both the C2,3 sites and the S atom. DBT4 and DBT5 were products involved in the former route while BT1 and BT2 were S oxidation products.

DD1 is a newly identified product of DD. Because this product did not accumulate, and no metabolite was detected in the DD angular dioxygenation pathway. DD2 was proposed to be produced through DD1 via a lateral dioxygenation and *meta*-cleavage pathway. When the halogenated compounds 4-BDE, 2-CDD, 4,4′-DCBP and 2,2′-DCBP were degraded, the corresponding products phenol and 4-bromophenol, 3-chlorocatechol, 4-chlorobenzoate and 2-chlorobenzoate were detected. The structural similarity of the produced phenol, catechol and benzoate,

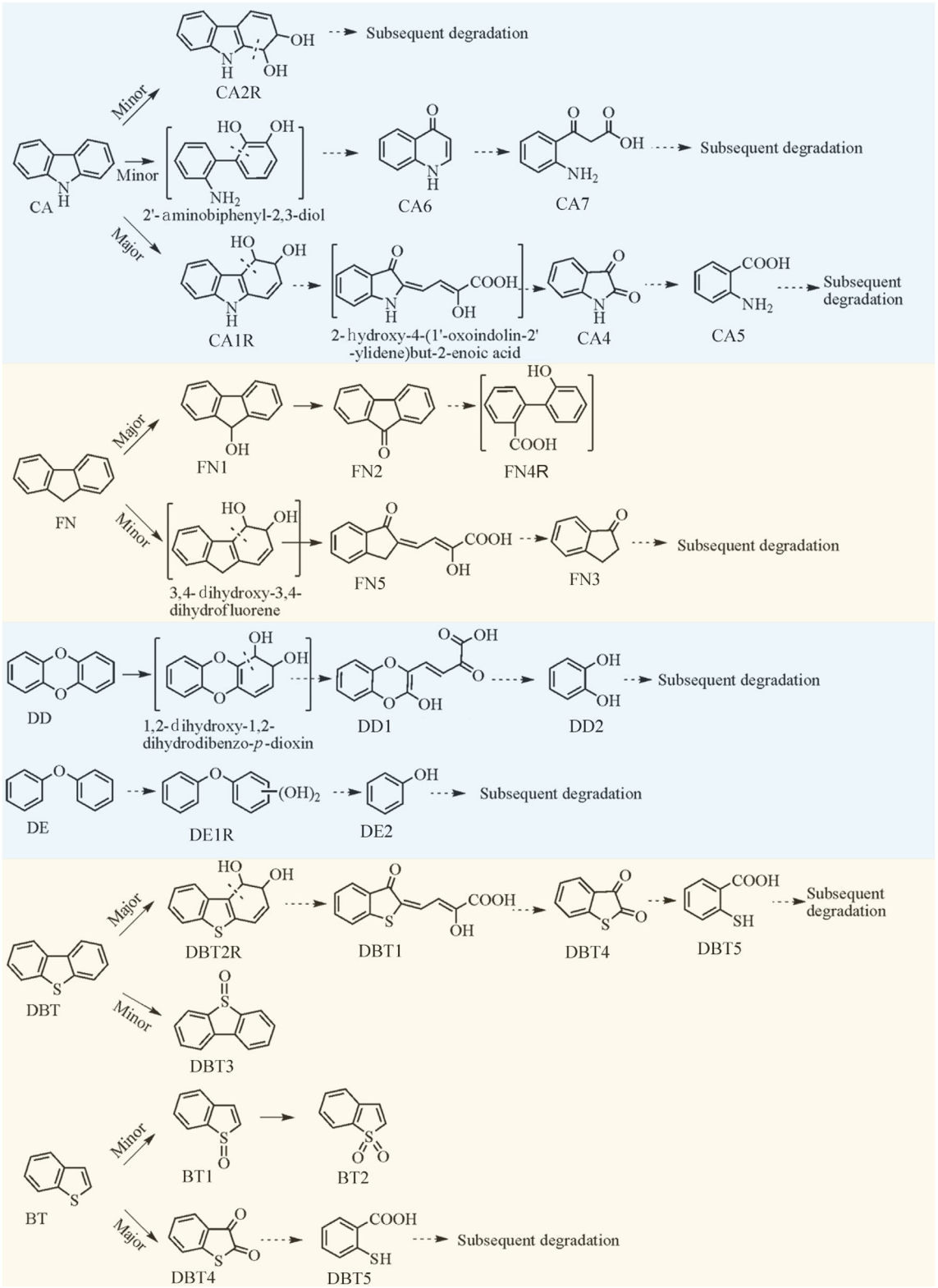

Fig 6. Legend on next page.

respectively, from DE, DD and BP, indicates that these halogenated derivatives and their respective non-halogenated models may be degraded following similar routes. The production of phenol and 4-bromophenol from 4-BDE means that 4-BDE can be transformed by cleavage of both the brominated and unsubstituted benzene rings.

BP-utilizing bacteria have been studied mostly because of their extensive PCB degradation abilities. Waldau *et al*. (2009) demonstrated the cometabolic transformation of CA, FN and DBT by 24 BP-utilizing bacteria. In most cases, the oxygenated substrates were detected as the main and end products. Oxygenation of DD and monochlorinated DD by a BP-utilizing *Beijerinckia* sp. strain has also been reported; further transformation products were not detected (Klecka and Gibson, 1980). In contrast, as shown in Fig. 6, strain B6-2 is capable of degrading these aromatic polycycles to single-ring aromatic compounds. They did not accumulate, and some of them including benzoate, anthranilate, salicylate and catechol were capable of supporting cell growth of strain B6-2, indicating that these PAHs and dioxins could be mineralized at least partially. This should be an advantage of strain B6-2 for degradation of aromatic compounds and their derivatives.

The abilities of strain B6-2 to deal with mixed aromatic polycycles and survive with extremely toxic organic solvents were tested. The degradation studies demonstrated that strain B6-2 could cometabolically degrade all 13 detected EPA-PAHs with 3–6 fused benzene rings, seven dioxins and six DBT/BT and their methyl derivatives. DBT/BT and their methyl derivatives were selected as models to examine their effects on cell growth of strain B6-2, and only a little inhibition was observed (Fig. 1I). Growth experiments demonstrated that B6-2 could survive with extremely toxic solvents at a volume ratio up to 20%. Growth of strain B6-2 with BP in MSM exposed to 0.5% *p*-xylene indicated that the enzymes corresponding to BP degradation were active in the presence of toxic solvents at a lethal volume. To our knowledge, strain B6-2 is the first studied wide-range aromatic polycycle-degrader capable of resisting organic solvents, which identifies B6-2 as a potential candidate to remediate extremely polluted environments.

Genetic analysis reveals genes responsible for the utilization of BP, benzoate, 4-hydroxybenzoate and salicylate, and solvent resistance of strain B6-2. These genes are always independently present in bacteria. Several bacteria such as *Burkholderia xenovorans* LB400 (Denef *et al*., 2005), *P. putida* KT2440 (Jiménez *et al*., 2002; Puchalka *et al*., 2008), *Rhodococcus jostii* RHA1 (Shimizu *et al*., 2001; Patrauchan *et al*., 2005) and *P. pseudoalcaligenes* KF707 (Fujihara *et al*., 2006) have more than one aromatic compound-degrading gene cluster. However, it has not been reported that a bacterium such as strain B6-2 has so many aromatic compound-degrading and efflux pumps gene clusters. Co-existence of various incorporated genes may be an adaptation mechanism for strain B6-2 to survive in the polluted environment where it was isolated (Boor, 2006). Each sequence of the enzymes relative to utilization of aromatic compounds and solvent tolerance from strain B6-2 shows the highest similarity (>90%) with those in GenBank. Therefore, the co-existence of those genes in strain B6-2 was most likely caused by lateral gene transfer, providing most of the diversity in genetic repertoires of γ-Proteobacteria including *Pseudomonas* spp. (Lerat *et al*., 2005).

Aromatic compound-degrading enzymes are always expressed after the induction by special effectors, aromatic compounds, or their metabolites. Proteome and transcriptome analyses reveal the expression of enzymes induced by BP responsible for the transformation of BP to benzoate, which is further mineralized via the catechol *ortho*-cleavage pathway (Fig. S7). The 4-hydroxybenzoate- and salicylate-degrading enzymes were not detected in cells of strain B6-2 using BP as a sole carbon source. However, because 4-hydroxybenzoate and salicylate are used as sole carbon sources by strain B6-2, these enzymes should be expressed under special environments, enabling B6-2 to pillage available aromatic carbon sources to survive.

Although various PAHs and dioxins are transformed, genetic and proteomic analyses reveal that B6-2 has only one gene cluster, *bphABC*, for the aromatic polycycle upper degradation pathways. Among the previously reported BP upper degradation pathway enzymes, only BphABC of LB400 were expressed in a recombinant *E. coli* strain and shown to be responsible for the production of HOBB from DBF (Seeger *et al*., 2001; Mohammadi and Sylvestre, 2005). BphA1 (the large subunit of the terminal dioxygenase of BphA) is crucial for the substrate

Fig 6. Catabolic pathways of CA, FN, DBT, BT, DD and DE by strain B6-2. Compounds in the brackets were not detected by direct or indirect evidence in our study and their involvement in the pathways were proposed according to the previous studies. The dashed arrows indicate two or more steps of reactions. CA1R, 3,4-dihydroxy-3,4-dihydrocarbazole; CA2R, 1,2-dihydroxy-1,2-dihydrocarbazole; CA4, isatin; CA5, anthranilate; CA6, 4-quinolinone; CA7, 3-(2-aminophenyl)-3-oxopropanoic acid; FN1, 9-fluorenol; FN2, 9-fluorenone; FN3, 1-indanone; FN4R, 2′-hydroxybiphenyl-2-carboxylic acid; FN5, 2-hydroxy-4-(1′-oxoinden-2′-ylidene)but-2-enoic acid; DD1, 4-(3-hydroxybenzo[b][1,4]dioxin-2-yl)-2-oxo-3-butenoic acid; DD2, catechol; DE1R, diphenyl ether-dihydrodiol; DE2, phenol; DBT1, 2-hydroxy-4-(3′-oxobenzothiophene-2′-ylidene)but-2-enoic acid; DBT2R, 1,2-dihydroxy-1,2-dihydrodibenzothiophene; DBT3, DBT-S-oxide; DBT4, BT-2,3-dione; DBT5, 2-mercaptobenzoate; BT1, BT-S-oxide; BT2, BT-S,S-dioxide.

ring of BphA which is a key enzyme of a BP-utilizing bacterium. A few changes of amino acids at the crucial sites between 234 and 377 of BphA1 can largely change the substrate ranges and oxygenation sites by BphA (Furukawa *et al*., 2004; Kumamaru *et al*., 1998). Although the BphA1 sequence of B6-2 has high similarities with those of the model strains LB400 and KF707 (90% and 92%, respectively) (Fig. S4), the major difference is concentrated between the amino acid sites 234 and 377, which should be a reason why B6-2 could transform a series of S, N and O heterocycles, PAHs and dioxins. LB400 could transform DBF but not CA or DBT (Haddock and Gibson, 1995), and KF707 could not transform DBF, CA, DBT, or FN (Misawa *et al*., 2002). Versatility of BphABC together with natural integration of those multiple functional genes should be major factors contributing to the versatility of strain B6-2.

P. putida has been shown to be biosafe based on phenotypic and genetic information. Therefore, it has been recognized as a host to develop a safe strain for environmental biotechnology and biotechnological production processes. Many potentially interesting biocatalytic conversions involving apolar substrates and products, such as aliphatic, aromatic and heterocyclic compounds were performed by solvent-tolerant *P. putida* (Tao *et al*., 2006; Puchalka *et al*., 2008; Wackett, 2003; Nijkamp *et al*., 2007; Timmis, 2002). Studies on mechanisms of aromatic chemical catabolism and solvent tolerance by *P. putida* B6-2 will facilitate rational manipulation of this strain for bioremediation and potentially establish it as a host to construct cell factories for biotechnology in the well-known aqueous-organic two-phase system. Overall, this bacterium strain B6-2 may be a useful model for studying biochemical, genetic, evolutionary and ecological aspects of *P. putida* in the environment.

Experimental procedures

Bacterial strain, media and culture conditions

P. putida strain B6-2 was isolated from a biphenyl polluted soil sample; it was deposited both at American Type Culture Collection (ATCC BAA-2545) and at Deutsche Sammlung von Mikroorganismen und Zellkulturen (DSM 28064). Mineral salt medium (MSM) is consisted of (g l^{-1}) 2.0 KH_2PO_4, 3.28 $Na_2HPO_4{\cdot}12H_2O$, 0.1 $MgSO_4$, 1.0 $(NH_4)_2SO_4$ and 0.00025 $FeCl_3$. Citrate medium used for the control group of the proteomic assay was composed of (g l^{-1}) 2.0 KH_2PO_4, 3.28 $Na_2HPO_4{\cdot}12H_2O$, 1.0 $(NH_4)_2SO_4$, 0.00025 $FeCl_3$, 0.1 $MgSO_4$ and 1.0 trisodium citrate. Cells were cultivated either in MSM with 15 mmol l^{-1} BP or in Luria-Bertani (LB) medium (tryptone 1%, yeast extract 0.5%, NaCl 1%, pH 7.5) or citrate medium at 30°C on a reciprocal shaker at 200 rpm. FN, CA, DD, 4-BDE, 4-MDBT, BT, *N*-methyl-*N*-nitrosourea, anthranilate, 1-indanone and chromatographic grade ethyl acetate were purchased from Sigma-Aldrich Chemical Co., Inc. DBT, DE, 4,4′-DBDE, 4,6-DMDBT, 5-MBT, 9-fluorenol, 9-fluorenone and isatin were purchased from ACROS Organic Co., Inc. 2-MBT and salicylate were obtained from Tokyo Kasei Kogyo Co., Ltd. The standard EPA-PAHs were purchased from AccuStandard (New Haven, CT). All other commercially available chemicals were of analytical grade.

Utilization of aromatic compounds as growth substrates

Growth of strain B6-2 in MSM with individual aromatic compounds as the sole source of carbon and energy was tested by demonstrating an increase in cell turbidity (OD_{620}) with a concomitant decrease in the concentration of each of the following substrates FN, CA, DBT, BT, DE and DD at 1 mmol l^{-1}, benzoate, salicylate and 4-hydroxybenzoate at 5 mmol l^{-1} and anthranilate and catechol at 2 mmol l^{-1}. Autoclaved cell-inoculated flasks and flasks without substrates served as controls. In every test, triplicate samples and controls were analysed.

Cometabolic degradation of aromatic compounds

BP-grown B6-2 cells at the late exponential phase were collected by centrifugation at 4120 × g for 15 min, washed three times, and resuspended in MSM to get a cell suspension with an OD_{620} of 5.0. In experiments dealing with the cometabolic degradation of individual aromatic compounds, FN, CA, DBT, BT, DE, DD, 2,2′-DCBP and 4.4′-DCBP were added separately to the cell suspension at a final concentration of 0.2 mmol l^{-1}. In experiments testing the cometabolic degradation of mixed aromatic compounds by the cell suspension, two kinds of mixtures were used. The first one was obtained by extracting several times using acetone from PAHs contaminated soil. Identification and determination of the amounts of 16 EPA-PAHs in the extract were performed by comparing their retention times, UV–Vis spectra, and peak areas in HPLC with those of the standard EPA-PAHs. The second one was a mixture of dioxins including 2,8-DCDF, 2-CDD, 4-BDE, 4,4′-DBDE, 3,4-DCBP, 4,4′-DCBP and 2,2′-DCBP; each was added to the cell suspension at a final concentration of 0.1 mmol l^{-1}. In experimental tests for the growth of strain B6-2 with BP and the concomitant degradation of DBT, 4-MDBT, 4,6-DMDBT, BT, 2-MBT and 5-MBT, the initial OD_{620} of the incubations was 0.15, and BP was added at a concentration of 15 mmol l^{-1}, while the others were at 0.1 mmol l^{-1} (Li *et al*., 2009). The above experiments were performed using autoclaved cell-inoculated flasks as controls. In every test, triplicate samples and controls were analysed.

Analytical methods

HPLC was carried out to analyse the degradation of single aromatic compound and the mixture of PAHs extracted from contaminated soil using an Agilent 1100 series (Hewlett-Packard) instrument equipped with a variable-wavelength detector and a reversed phase C18 column (250 mm × 4.6 mm × 5 μm; Hewlett-Packard). The samples with single substrate were prepared by adding two volumes of ethanol to the whole cultures, followed by centrifugation (12,000 rpm for 10 min) and filtration. The samples with the mixture of extracted PAHs were prepared by extracting the whole cultures three times with equal volume of ethyl acetate, and subsequently concentrating the extracts to a small volume. In some cases, the major metabolites were prepared by using HPLC and analysed with HPLC–MS of an API 4000 LC–MS–MS system (Applied Biosystems, Foster City, CA).

GC was performed to detect the degradation of the mixed dioxins, DBT/BTs and their derivatives by strain B6-2, and the mixed PAHs and dioxins by the transformants using a SPB-5 column (0.32 mm i.d. × 30 m length; Supelco) connected to a flame ionization detector (FID, CP3380, Varian Associates) with nitrogen gas as the carrier gas. Samples were prepared similarly as the preparation of the samples with the mixture of extracted PAHs.

GC–MS (GCD 1800C, Hewlett-Packard) was carried out using a 50 m DB-5 MS column (J&W Scientific Folsom, CA). The oven temperature program started at 60°C for 6 min, and then ramped to 150°C at 10°C/min, and to 280°C at 15°C/min, which was kept for 6 min.

Identification of metabolites

The BP degradation metabolites were extracted with ethyl acetate from the supernatant of the culture with BP as the sole carbon source after acidification to pH 2.0 with 1.25 mol l^{-1} H_2SO_4. The extracts were dried with Na_2SO_4, evaporated under nitrogen gas and analysed using GC–MS. FN, CA, DBT, BT, DD, DE, 4-BDE, 2-CDD, 4,4′-DCBP and 2,2′-DCBP were separately added to the cell suspension with OD_{620} of 5.0 at a final concentration of 0.5 mmol l^{-1}. At incubation time for 12 h and 24 h, half of each culture was sampled and centrifuged. Metabolites were prepared similarly to the process for preparing BP metabolites. Thereafter, the samples were derivatized with an ethereal solution of diazomethane, which was generated from N-methyl-N-nitroso-N-nitroguanidine according to a previously reported method (Arensdorf and Focht, 1995) and then analysed by GC–MS.

Growth of strain B6-2 under the stress of solvents

After pre-growth in LB medium with 0.3% (V/V) of *p*-xylene, the growth of strain B6-2 was tested in LB medium plus 20% (V/V) of each following organic solvent (log P_{ow}): *n*-decane (5.6), *n*-heptane (4.1), *p*-xylene (3.1), toluene (2.5) and benzene (2), respectively. In another experiment, growth of strain B6-2 with 15 mmol l^{-1} BP in MSM exposed to 0.5% (V/V) of *p*-xylene was monitored.

Analysis of 2-D gels and protein identification

Analysis of the resulting 2-D gel images, including spot detection and matching was performed with the software PDQuest 7.2 (Bio-Rad). The background subtraction was made in a rectangle that completely enclosed each spot, with a local correction mode. All the protein spots whose intensities were at least fivefold higher in BP-grown cells versus the control (sodium citrate-grown cells) were excised from stained gels and washed twice in 0.5 ml water for 10 min, then in 50 μl of 25 mmol l^{-1} NH_4HCO_3 resolved in water-acetonitrile (50%, V/V) for 30 min, and then in 50 μl of acetonitrile for 5 min. The gel pieces were then dried in a vacuum freeze drier (Thermo savant) and swollen in 3 μl of digestion solution (25 mM NH_4HCO_3 containing 0.01 μg μl^{-1} trypsin) at 4°C for 1 h. Then, 10 μl of 25 mM NH_4HCO_3 was added. After incubation at 37°C overnight, digestion was stopped with 0.1% TFA. Peptide spectra were obtained by MALDI-TOF-MS (AXIMA-CFR Plus, SHIMADSU) in the positive-ion reflector mode with saturated alpha-cyano-4-hydroxycinnamic acid as the matrix. After the spectra were internally calibrated by means of trypsin autolysis products, the obtained peptide statistical analysis mass fingerprint was used to search through the SWISS-PROT and NCBInr databases by using the MASCOT search engine (www.matrixscience.com) and the databases generated by in silico digestion of the total proteomes of *P. putida* strains F1, KT2440, GB-1, W619 and *Burkholderia xenovorans* strain LB400 by using the software General Protein/Mass Analysis for Windows. Searches were performed allowing for the following modifications: carbamidomethylation of cysteine, partial oxidation of methionine residues and up to one missed trypsin cleavage. A protein was considered identified if the search score was above 75 and predicted molecular mass and isoelectric point values were consistent with the experimentally determined ones. Theoretical molecular masses and isoelectric points of the proteins were calculated.

Genome sequencing of strain B6-2

Genomic DNA of strain B6-2 was extracted using Wizard Genomic Purification Kit (Promega, USA). The genome

of B6-2 was sequenced on the single molecule real-time (SMRT) DNA sequencing platform by Pacific Biosciences (PacBio) RS II sequencer. The raw data were *de novo* assembled using the hierarchical genome-assembly process (HGAP) protocol (Version 2.3) (Chin *et al*., 2013), and resulted in one circularized complete chromosome sequence, with about 300-fold coverage. The coding sequences, tRNA and rRNA were annotated using the RAST server (Aziz *et al*., 2008). Clean sequences were functionally annotated by the Rapid Annotations using Subsystems Technology (RAST) annotation server. The whole genome shotgun project was deposited in GenBank under the accession number CP015202.1.

BphA1, the α-subunit of biphenyl 2,3-dioxygenases, in strains B356, RHA1, B6-2, KF707 and LB400 were analysed by CLUSTER 2.1 MULTIPLE SEQUENCE ALIGNENT. SWISS-MODEL was used to conduct homology modelling of BphA1 in strain B6-2, and the most similar protein (5AEU) was selected in the PDB database as the template. The structure model-B6-2 obtained by homology modelling was docked with the small PAHs molecules (biphenyl, dibenzofuran, carbazole, dibenzothiophene, fluorene, diphenyl oxide, dibenzo-*p*-dioxin), and the structure with the highest score was selected as the final docking result. We use the software Discovery Studio to view ligand-protein interactions and get a series of amino acids that have interactions with the substrate.

Preparation for proteomic and RNA-seq assays

Strain B6-2 was grown in 15 mmol l^{-1} BP-MSM or MIX (BP/CA/DBF/DBT)-MSM was prepared as the treatment group. Cells grown with trisodium citrate (TSC) in MSM were prepared as the control group. Samples were collected at mid-exponential phase. All samples were stored at −80°C after being frozen in liquid nitrogen. Then, all samples of both groups were treated as described previously (Tang *et al*., 2013). The proteomic assay was conducted by multidimensional liquid chromatography using an 1100 LC system coupled with an LTQ Classic ion trap mass spectrometer (Thermo Fisher), and RNA-seq was performed by Shanghai Personal Biotechnology Co.

Acknowledgements

This study was supported by grants from National Key Research and Development Project (2018YFA0901200), National Natural Science Foundation of China (21777098 and 32000062), Chinese National Science Foundation for Excellent Young Scholars (31422004), Shanghai Excellent Academic Leaders Program (20XD1421900) and Shuguang Program (17SG09) that is supported by the Shanghai Education Development Foundation and Shanghai Municipal Education Commission.

Conflict of Interest

The authors declare no competing financial interests.

Author Contributions

Weiwei Wang, Qinggang Li, Hongzhi Tang and Ping Xu conceived the projects and wrote the manuscript. Weiwei Wang, Hongzhi Tang, Qinggang Li and Lige Zhang designed and performed all the experiments. Weiwei Wang, Hongzhi Tang, Jie Cui, Hao Yu, Xingyu Ouyang, Xiaoyu Wang and Fei Tao analysed the results.

References

Arensdorf, J.J., and Focht, D.D. (1995) A *meta* cleavage pathway for 4-chlorobenzoate, an intermediate in the metabolism of 4-chlorobiphenyl by *Pseudomonas cepacia* P166. *Appl Environ Microbiol* **61**: 443–447.

Aziz, R.K., Bartels, D., Best, A.A., DeJongh, M., Disz, T., Edwards, R.A., *et al*. (2008) The RAST server: rapid annotations using subsystems technology. *BMC Genomics* **9**: 75.

Blumenstock, M., Zimmermann, R., Schramm, K.W., and Kettrup, A. (2000) Influence of combustion conditions on the PCDD/F-, PCB-, PCBz- and PAH-concentrations in the post-combustion chamber of a waste incineration pilot plant. *Chemosphere* **40**: 987–993.

Boor, K.J. (2006) Bacterial stress responses: what doesn't kill them can make them stronger. *PLoS Biol* **4**: e23.

Bressler, D.C., and Fedorak, P.M. (2001) Identification of disulfides from the biodegradation of dibenzothiophene. *Appl Environ Microbiol* **67**: 5084–5093.

Camara, B., Herrera, C., Gonzalez, M., Couve, E., Hofer, B., and Seeger, M. (2004) From PCBs to highly toxic metabolites by the biphenyl pathway. *Environ Microbiol* **6**: 842–850.

Chang, Y.S. (2008) Recent developments in microbial biotransformation and biodegradation of dioxins. *J Mol Microbiol Biotechnol* **15**: 152–171.

Chin, C.S., Alexander, D.H., Marks, P., Klammer, A.A., Drake, J., Heiner, C., *et al*. (2013) Nonhybrid, finished microbial genome assemblies from long-read SMRT sequencing data. *Nat Methods* **10**: 563–569.

Denef, V.J., Patrauchan, M.A., Florizone, C., Park, J., Tsoi, T.V., Verstraete, W., *et al*. (2005) Growth substrate- and phase-specific expression of biphenyl, benzoate, and C1 metabolic pathways in *Burkholderia xenovorans* LB400. *J Bacteriol* **187**: 7996–8005.

Dudhagara, D.R., and Dave, B.P. (2018) Mycobacterium—Research and development (Chapter 17). In *Mycobacterium as Polycyclic Aromatic Hydrocarbons (PAHs) Degrader*. London: IntechOpen Limited.

Eaton, R.W., and Nitterauer, J.D. (1994) Biotransformation of benzothiophene by isopropylbenzene-degrading bacteria. *J Bacteriol* **176**: 3992–4002.

Fujihara, H., Yoshida, H., Matsunaga, T., Goto, M., and Furukawa, K. (2006) Cross-regulation of biphenyl- and -salicylate-catabolic genes by two regulatory systems in

Pseudomonas pseudoalcaligenes KF707. *J Bacteriol* **188**: 4690–4697.

Furukawa, K., Suenaga, H., and Goto, M. (2004) Biphenyl dioxygenases: functional versatilities and directed evolution. *J Bacteriol* **186**: 5189–5196.

Gai, Z., Yu, B., Li, L., Wang, Y., Ma, C., Feng, J., *et al*. (2007) Cometabolic degradation of dibenzofuran and dibenzothiophene by a newly isolated carbazole-degrading *Sphingomonas* sp. strain. *Appl Environ Microbiol* **73**: 2832–2838.

Ghosal, D., Ghosh, S., Dutta, T.K., and Ahn, Y. (2016) Current state of knowledge in microbial degradation of polycyclic aromatic hydrocarbons (PAHs): a review. *Front Microbiol* **7**: 1369.

Grifoll, M., Selifonov, S.A., Gatlin, C.V., and Chapman, P.J. (1995) Actions of a versatile fluorene-degrading bacterial isolate on polycyclic aromatic compounds. *Appl Environ Microbiol* **61**: 3711–3723.

Gullett, B.K., Touati, A., and Hays, M.D. (2003) PCDD/F, PCB, HxCBz, PAH, and PM emission factors for fireplace and woodstove combustion in the San Francisco Bay region. *Environ Sci Technol* **37**: 1758–1765.

Habe, H., Ide, K., Yotsumoto, M., Tsuji, H., Yoshida, T., Nojiri, H., *et al*. (2002) Degradation characteristics of a dibenzofuran-degrader *Terrabacter* sp. strain DBF63 toward chlorinated dioxins in soil. *Chemosphere* **48**: 201–207.

Habe, H., and Omori, T. (2003) Genetics of polycyclic aromatic hydrocarbon metabolism in diverse aerobic bacteria. *Biosci Biotechnol Biochem* **67**: 225–243.

Haddock, J.D., and Gibson, D.T. (1995) Purification and characterization of the oxygenase component of biphenyl 2,3-dioxygenase from *Pseudomonas* sp. strain LB400. *J Bacteriol* **177**: 5834–5839.

Harwood, C.S., Nichols, N.N., Kim, M.K., Ditty, J.L., and Parales, R.E. (1994) Identification of the pcaRKF gene cluster from *Pseudomonas putida*: involvement in chemotaxis, biodegradation, and transport of 4-hydroxybenzoate. *J Bacteriol* **176**: 6479–6488.

Hennessee, C.T., and Li, Q.X. (2016) Effects of polycyclic aromatic hydrocarbon mixtures on degradation, gene expression, and metabolite production in four *Mycobacterium* species. *Appl Environ Microbiol* **82**: 3357–3369.

Iida, T., Nakamura, K., Izumi, A., Mukouzaka, Y., and Kudo, T. (2006) Isolation and characterization of a gene cluster for dibenzofuran degradation in a new dibenzofuran-utilizing bacterium, *Paenibacillus* sp. strain YK5. *Arch Microbiol* **184**: 305–315.

Inoue, A., and Horikoshi, K. (1989) A *Pseudomonas* thrives in high concentrations of toluene. *Nature* **338**: 3.

Inoue, K., Habe, H., Yamane, H., and Nojiri, H. (2006) Characterization of novel carbazole catabolism genes from gram-positive carbazole degrader *Nocardioides aromaticivorans* IC177. *Appl Environ Microbiol* **72**: 3321–3329.

Isken, S., and de Bont, J.A. (1998) Bacteria tolerant to organic solvents. *Extremophiles* **2**: 229–238.

Isken, S., Derks, A., Wolffs, P.F., and de Bont, J.A. (1999) Effect of organic solvents on the yield of solvent-tolerant *Pseudomonas putida* S12. *Appl Environ Microbiol* **65**: 2631–2635.

Jiménez, J.I., Miñambres, B., García, J.L., and Diaz, E. (2002) Genomic analysis of the aromatic catabolic pathways from *Pseudomonas putida*, KT2440. *Environ Microbiol* **4**: 824–841.

Jiménez, J.I., Pérez-Pantoja, D., Chavarría, M., Díaz, E., and de Lorenzo, V. (2014) A second chromosomal copy of the *catA* gene endows *Pseudomonas putida* mt-2 with an enzymatic safety valve for excess of catechol. *Environ Microbiol* **16**: 1767–1778.

Keith, L.H., and Telliard, W.A. (1979) Priority pollutants. I. A perspective view. *Environ Sci Technol* **13**: 416–423.

Klecka, G.M., and Gibson, D.T. (1980) Metabolism of dibenzo-*p*-dioxin and chlorinated dibenzo-*p*-dioxins by a *Beijerinckia* species. *Appl Environ Microbiol* **39**: 288–296.

Kim, E., and Zylstra, G.J. (1995) Molecular and biochemical characterization of two *meta*-cleavage dioxygenases involved in biphenyl and *m*-xylene degradation by *Beijerinckia* sp. strain B1. *J Bacteriol* **177**: 3095–3103.

Kieboom, J., Dennis, J.J., de Bont, J.A., and Zylstra, G.J. (1998) Identification and molecular characterization of an efflux pump involved in *Pseudomonas putida* S12 solvent tolerance. *J Biol Chem* **273**: 85–91.

Kropp, K.G., and Fedorak, P.M. (1998) A review of the occurrence, toxicity, and biodegradation of condensed thiophenes found in petroleum. *Can J Microbiol* **44**: 605–622.

Kumamaru, T., Suenaga, H., Mitsuoka, M., Watanabe, T., and Furukawa, K. (1998) Enhanced degradation of polychlorinated biphenyls by directed evolution of biphenyl dioxygenase. *Nat Biotechnol* **16**: 663–666.

Lerat, E., Daubin, V., Ochman, H., and Moran, N.A. (2005) Evolutionary origins of genomic repertoires in bacteria. *PLoS Biol* **3**: e130.

Li, L., Li, Q., Li, F., Shi, Q., Yu, B., Liu, F., *et al*. (2006) Degradation of carbazole and its derivatives by a *Pseudomonas* sp. *Appl Microbiol Biotechnol* **73**: 941–948.

Li, Q., Wang, X., Yin, G., Gai, Z., Tang, H., Ma, C., *et al*. (2009) New metabolites in dibenzofuran cometabolic degradation by a biphenyl-cultivated *Pseudomonas putida* strain B6-2. *Environ Sci Technol* **43**: 8635–8643.

Lu, X.Y., Zhang, T., and Fang, H.H. (2011) Bacteria-mediated PAH degradation in soil and sediment. *Appl Microbiol Biotechnol* **89**: 1357–1371.

Lu, X.Y., Wang, W.W., Zhang, L.G., Hu, H.Y., Xu, P., Wei, T., *et al*. (2019) Molecular mechanism of N,N-dimethylformamide degradation in *Methylobacterium* sp. strain DM1. *Appl Environ Microbiol* **85**: e00275–e00219.

Ma, Y.F., Wang, L., and Shao, Z.Z. (2006) *Pseudomonas*, the dominant polycyclic aromatic hydrocarbon-degrading bacteria isolated from Antarctic soils and the role of large plasmids in horizontal gene transfer. *Environ Microbiol* **8**: 455–465.

Misawa, N., Shindo, K., Takahashi, H., Suenaga, H., Iguchi, K., Okazakiet, H., *et al*. (2002) Hydroxylation of various molecules including heterocyclic aromatics using recombinant *Escherichia coli* cells expressing modified biphenyl dioxygenase genes. *Tetrahedron* **58**: 9605–9612.

Mohammadi, M., and Sylvestre, M. (2005) Resolving the profile of metabolites generated during oxidation of dibenzofuran and chlorodibenzofurans by the biphenyl catabolic pathway enzymes. *Chem Biol* **12**: 835–846.

Nijkamp, K., Westerhof, R.G., Ballerstedt, H., de Bont, J.A., and Wery, J. (2007) Optimization of the solvent-tolerant *Pseudomonas putida* S12 as host for the production of *p*-coumarate from glucose. *Appl Microbiol Biotechnol* **74**: 617–624.

Nojiri, H., Nam, J.W., Kosaka, M., Morii, K.I., Takemura, T., Furihataet, K., *et al*. (1999) Diverse oxygenations catalyzed by carbazole 1,9a-dioxygenase from *Pseudomonas* sp.strain CA10. *J Bacteriol* **181**: 3105–3113.

Nojiri, H., Sekiguchi, H., Maeda, K., Urata, M., Nakai, S., Yoshidaet, T., *et al*. (2001) Genetic characterization and evolutionary implications of a *car* gene cluster in the carbazole degrader *Pseudomonas* sp. strain CA10. *J Bacteriol* **183**: 3663–3679.

Patrauchan, M.A., Florizone, C., Dosanjh, M., Mohn, W.W., Davies, J., and Eltis, L.D. (2005) Catabolism of benzoate and phthalate in *Rhodococcus* sp. strain RHA1: redundancies and convergence. *J Bacteriol* **187**: 4050–4063.

Peng, R.H., Xiong, A.S., Xue, Y., Fu, X.Y., Gao, F., Zhao, W., *et al*. (2008) Microbial biodegradation of polyaromatic hydrocarbons. *FEMS Microbiol Rev* **32**: 927–955.

Perera, F., Tang, W.Y., Herbstman, J., Tang, D., Levin, L., Miller, R., *et al*. (2009) Relation of DNA methylation of 5′-CpG island of ACSL3 to transplacental exposure to airborne polycyclic aromatic hydrocarbons and childhood asthma. *PLoS One* **4**: e4488.

Puchalka, J., Oberhardt, M.A., Godinho, M., Bielecka, A., Regenhardt, D., Timmis, K.N., *et al*. (2008) Genome-scale reconstruction and analysis of the *Pseudomonas putida* KT2440 metabolic network facilitates applications in biotechnology. *PLoS Comput Biol* **4**: e1000210.

Qu, Y., Ma, Q., Liu, Z., Wang, W.W., Tang, H.Z., Zhou, J.T., *et al*. (2017) Unveiling the biotransformation mechanism of indole in a *Cupriavidus* sp. strain. *Mol Microbiol* **106**: 905–918.

Sampedro, I., Rarales, R.E., Krell, T., and Hill, J.E. (2014) *Pseudomonas* chemotaxis. *FEMS Microbiol Rev* **39**: 17–46.

Schneider, J., Grosser, R.J., Jayasimhulu, K., Xue, W., Kinkle, B., and Warshawsky, D. (2000) Biodegradation of carbazole by *Ralstonia* sp. RJGII.123 isolated from a hydrocarbon contaminated soil. *Can J Microbiol* **46**: 269–277.

Schecter, A., Birnbaum, L., Ryan, J.J., and Constable, J.D. (2006) Dioxins: an overview. *Environ Res* **101**: 419–428.

Seeger, M., Camara, B., and Hofer, B. (2001) Dehalogenation, denitration, dehydroxylation, and angular attack on substituted biphenyls and related compounds by a biphenyl dioxygenase. *J Bacteriol* **183**: 3548–3555.

Seeger, M., and Pieper, D.H. (2010) *Genetics of Biphenyl Biodegradation and Co-metabolism of PCBs*, Berlin, Heidelberg: Springer, Vol. **2010**, pp. 1179–1199.

Shimizu, S., Kobayashi, H., Masai, E., and Fukuda, M. (2001) Characterization of the 450-kb linear plasmid in a polychlorinated biphenyl degrader, *Rhodococcus* sp. strain RHA1. *Appl Environ Microbiol* **67**: 2021–2028.

Tang, H.Z., Yu, H., Li, Q.G., Wang, X.Y., Gai, Z.H., Yin, G. B., *et al*. (2011) Genome sequence of *Pseudomonas putida* strain B6-2, a superdegrader of polycyclic aromatic hydrocarbons and dioxin-like compounds. *J Bacteriol* **193**: 6789–6790.

Tang, H.Z., Wang, L.J., Wang, W.W., Yu, H., Zhang, Z.Z., Yao, Y.X., *et al*. (2013) Systematic unraveling of the unsolved pathway of nicotine degradation in *Pseudomonas*. *PLoS Genet* **9**: e1003923.

Tao, F., Yu, B., Xu, P., and Ma, C.Q. (2006) Biodesulfurization in biphasic systems containing organic solvents. *Appl Environ Microbiol* **72**: 4604–4609.

Timmis, K.N. (2002) *Pseudomonas putida*: a cosmopolitan opportunist par excellence. *Environ Microbiol* **4**: 779–781.

van Herwijnen, R., Wattiau, P., Bastiaens, L., Daal, L., Jonker, L., Springael, D., *et al*. (2003) Elucidation of the metabolic pathway of fluorene and cometabolic pathways of phenanthrene, fluoranthene, anthracene and dibenzothiophene by *Sphingomonas* sp. LB126. *Res Microbiol* **154**: 199–206.

Wackett, L.P. (2003) *Pseudomonas putida*—a versatile biocatalyst. *Nat Biotechnol* **21**: 136–138.

Waldau, D., Methling, K., Mikolasch, A., and Schauer, F. (2009) Characterization of new oxidation products of 9H-carbazole and structure related compounds by biphenyl-utilizing bacteria. *Appl Microbiol Biotechnol* **81**: 1023–1031.

Wierckx, N.J., Ballerstedt, H., de Bont, J.A., and Wery, J. (2005) Engineering of solvent-tolerant *Pseudomonas putida* S12 for bioproduction of phenol from glucose. *Appl Environ Microbiol* **71**: 8221–8227.

Wittich, R.M. (1998) Degradation of dioxin-like compounds by microorganisms. *Appl Microbiol Biotechnol* **49**: 489–499.

Xu, P., Yu, B., Li, F.L., Cai, X.F., and Ma, C.Q. (2006) Microbial degradation of sulfur, nitrogen and oxygen heterocycles. *Trends Microbiol* **14**: 398–405.

Yamazoe, A., Yagi, O., and Oyaizu, H. (2004) Biotransformation of fluorene, diphenyl ether, dibenzo-*p*-dioxin and carbazole by *Janibacter* sp. *Biotechnol Lett* **26**: 479–486.

Yao, X.M., Tao, F., Zhang, K.Z., Tang, H.Z., and Xu, P. (2017) Multiple roles of two efflux pumps in a polycyclic aromatic hydrocarbon-degrading *Pseudomonas putida* strain B6-2 (DSM 28064). *Appl Environ Microbiol* **83**: e01882–e01817.

Yao, X.M., Tao, F., Tang, H.Z., Hu, H.Y., Wang, W.W., and Xu, P. (2020) Unique regulator SrpR mediates crosstalk between efflux pumps TtgABC and SrpABC in *Pseudomonas putida* B6-2 (DSM 28064). *Mol Microbiol* **115**: 131–141.

Supporting Information

Additional Supporting Information may be found in the online version of this article at the publisher's web-site:

Appendix S1. Supporting Information.